

Preparation of Different WO₃ Nanostructures and Comparison of Their Ability for Congo Red Photo Degradation

Alaei, Mahshad*⁺

Nanotechnology Research Center, Research Institute of Petroleum Industry (RIPI),
P.O. Box 14665-1998 Tehran, I.R. IRAN

Mahjoub, Ali Reza

Department of Chemistry, Faculty of Science, Tarbiat Modares University (TMU),
P.O. Box 14115-336 Tehran, I.R. IRAN

Rashidi, Alimorad

Nanotechnology Research Center, Research Institute of Petroleum Industry (RIPI),
P.O. Box 14665-1998 Tehran, I.R. IRAN

ABSTRACT: Tungsten trioxide nanoparticles with monoclinic structure and average particle size about 80 nm were prepared by the spray pyrolysis method. WO₃ nanorods with hexagonal structure and average dimension about 15 × 100 nm were synthesized in gram quantities by modified hydrothermal method at lower temperature and shorter reaction time in comparison to the previous research. Photo degradation of Congo Red showed that the as-prepared WO₃ nanoparticles is more effective than nanorod structure. WO₃ nanorods actually had no effect in Congo Red photo degradation. Therefore in this reaction, spherical morphology is superior to column morphology. The samples were characterized with X-Ray Diffraction (XRD), Scanning Electron Microscopy (SEM), EDX analysis, UV-visible spectrum and Transmission Electron Microscopy (TEM).

KEY WORDS: WO₃, Nanoparticle, Nanorod, Hydrothermal, Photo catalyst.

INTRODUCTION

Photo catalytic degradation of environmental pollutants of water or air by semiconducting materials has attracted extensive attentions during recent 20 years [1]. Many different semiconductors, such as TiO₂, SnO₂, WO₃, ZnO, Fe₂O₃, CdS, ZnS, and SrTiO₃ have been used as photo catalysts for the photo degradation of organic or inorganic pollutants [2-9].

Tungsten trioxide (WO₃) is a wide band gap semiconductor metallic oxide. This material has been used to detect

Different oxidizing and reducing gases [10-12]. It is applicable as catalyst, in windows for solar cells, electronic information displays and color memory devices [13-17].

WO₃ nanostructures can be prepared by different techniques such as thermal evaporation [18-20], sputtering [21-23], chemical vapor deposition [24], electro deposition [25] and sol-gel deposition [26]. The spray pyrolysis technique for material synthesis

* To whom correspondence should be addressed.

+ E-mail: alaiem@ripi.ir

1021-9986/12/1/31

7/\$/2.70

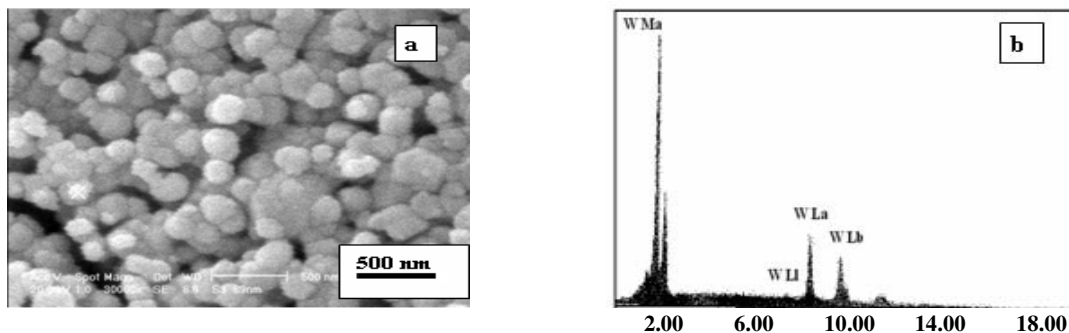


Fig. 1: a) SEM image and b) EDX analysis of the as-prepared WO_3 nanoparticles that were prepared by spray pyrolysis method.

is the most economical method and an interesting option due to the use of inexpensive precursor materials, low-cost equipments and its relative ease in preparing the large scale of nanomaterials.

In this work, two different morphologies of WO_3 nanostructures were prepared. The as-prepared WO_3 nanoparticles that were prepared with spray pyrolysis method are spherical shape with monoclinic structure and average size about 80 nm. WO_3 nanorods with hexagonal structure and average dimension about 15×100 nm were synthesized in gram quantities by modified hydrothermal method at lower temperature (160°C) and shorter reaction time (3 days) in comparison to the previous research [27].

The as-prepared samples were used as photo catalyst in Congo Red photo degradation. For this reaction, results showed that the spherical morphology is superior to the column morphology.

EXPERIMENTAL SECTION

Materials

All chemicals were of analytical grade and used without further purification.

Preparation of WO_3 nanoparticles

The spray process was done with a stainless-steel atomizer. Aqueous solution of ammonium para tungstate (for example 1.6 wt %) together a suitable organic additive (such as citric acid) at $\text{pH}=7$ was sprayed to the vertical furnace by using compressed air as carrier gas.

Preparation of WO_3 nanorods

Typically an aqueous solution of 1.32 g ammonium para tungstate ($(\text{NH}_4)_{10}\text{W}_{12}\text{O}_{41} \cdot 7\text{H}_2\text{O}$) and 2.1 g citric acid was heated around 120°C together mixing for 6-7 h until

a gel was formed. 2.45 g of hexadecyl amine dissolved in ethanol (together the suitable surfactant such as Triton X-100) was added to the gel and stirred for 15 h. The resulting mixture was transferred to a Teflon autoclave with a stainless steel protective outer body and heated at 160°C for 3 days together mixing. The product was washed with ethanol, cyclohexene, water and finally with ethanol and dried at room temperature.

Characterization

The samples were characterized by Scanning Electron Microscopy (SEM) using a Holland Phillips XL30 microscope. XRD patterns of the sample were recorded in ambient air using a Holland Phillips X-ray powder diffraction ($\text{Cu K}\alpha$, $\lambda=1.5406 \text{ \AA}$), at scanning speed of $2^\circ/\text{min}$ from 20° to 80° . UV-visible spectrums were prepared by Shimadzu analytical equipment (UV-2100). TEM image of the sample was prepared by Philips Analytical equipment (CM 200).

Congo red photo degradation

100 mL Congo Red aqueous solution (5 ppm) together with 0.1 g photo catalyst was illuminated with UV radiation in the presence of the air bubbles. Each 30 min., 4 mL sample was separated, centrifuged for removal of catalyst and characterized with UV-visible spectrometer.

RESULTS AND DISCUSSIONS

Preparation of WO_3 nanoparticles

SEM image was used to investigate the microscopic structure of the samples. Fig. 1(a) illustrates SEM image of the as-prepared WO_3 nanoparticles and indicates that the most of nanoparticles are spherical shape.

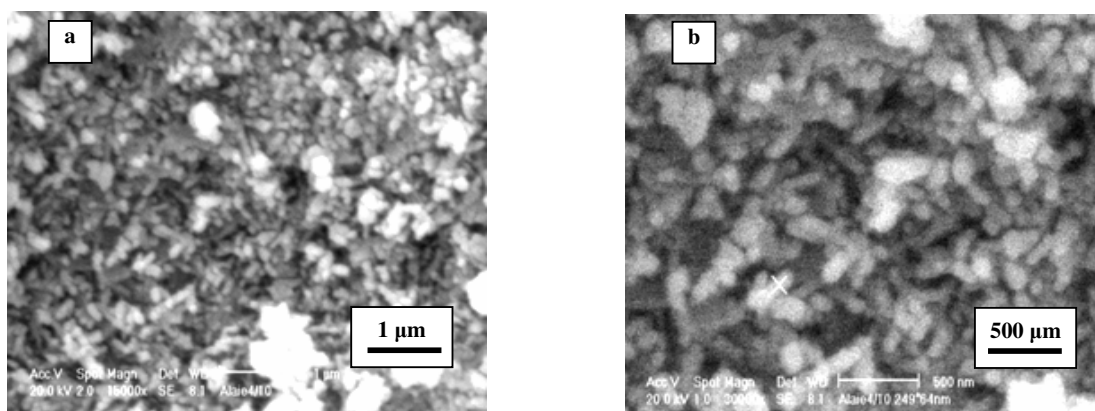


Fig. 2: SEM image of WO_3 nanorods (with two different scales) that were prepared by modified hydrothermal method.

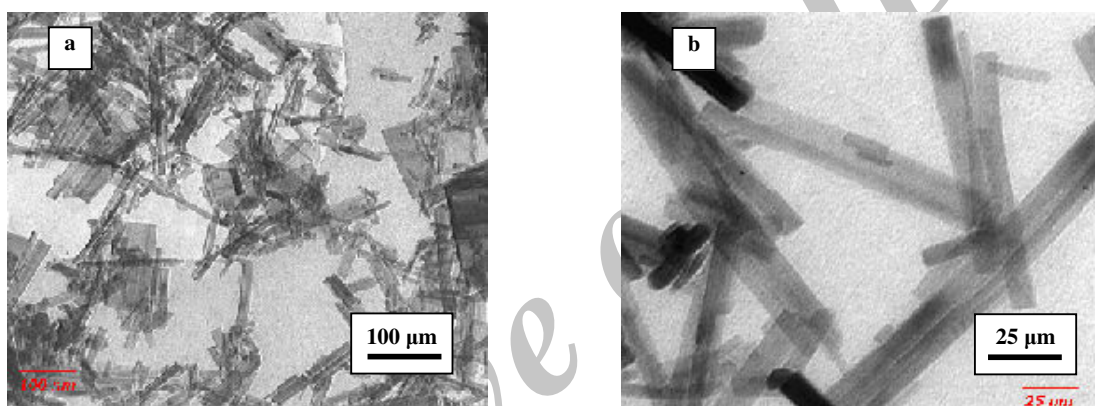


Fig. 3: TEM images of WO_3 nanorods (with two different scales) that were prepared by modified hydrothermal method.

In order to find chemical composition of the particles, EDX analyze was carried out. Fig. 1(b) shows the EDX analysis of the WO_3 nanoparticles that was prepared by spray pyrolysis method. It was observed just W element with no remarkable impurity.

XRD analysis was carried out to discover the crystalline phase and structure of the as-prepared WO_3 nanoparticles. Fig. 4 represents the XRD spectrum of the as-prepared WO_3 nanoparticles and formation of tungsten trioxide with monoclinic structure. The obtained spectrum has the first three WO_3 main peaks at $2\theta = 23.1, 24.4, 26.6$, in good agreement with the JCPDS 05-0363 standard card with $a = 7.28 \text{ \AA}$, $c = 3.83 \text{ \AA}$. The average particle size of the WO_3 nanoparticles was calculated from XRD pattern by Debye-Scherrer formula.

Preparation of WO_3 nanorods

Fig. 2 illustrates SEM image of the as-prepared WO_3 nanorods and Fig. 3 represents TEM image of them. These images show that the WO_3 nanorods with obviously individual morphology with average dimensions about $15 \times 100 \text{ nm}$ were prepared.

Addition of TX-100 as surfactant reduced the reaction temperature from 180°C to 160°C and the reaction time from 7 to 3 days in comparison to the previous research [27]. TX-100 facilitates the formation of individual and well defined WO_3 nanorods. There are definitely some interactions between the metal ions with the polar head groups of the surfactant (TX-100). These interactions may be the reason why WO_3 nanorods can form in better conditions such as lower temperature and shorter reaction time. It can be concluded that nucleation and growth are well controlled.

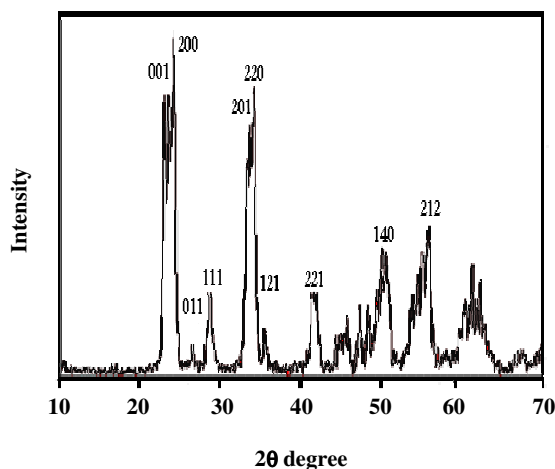


Fig. 4: XRD pattern of WO_3 nanoparticles that were prepared by spray pyrolysis method and indicates monoclinic structure.

XRD analysis was carried out to discover the crystalline phase and structure of the as-prepared WO_3 nanorods. Fig. 5 demonstrates the XRD pattern of the as-prepared WO_3 nanorods and the formation of tungsten trioxide with hexagonal structure. The obtained spectrum is in good agreement with the JCPDS 33-1387 standard card with $a = 7.29 \text{ \AA}$, $c = 3.89 \text{ \AA}$.

Congo Red photo degradation

WO_3 is known to be a photo catalytic material. In this paper, the photo catalytic activity of WO_3 nanostructures was measured by photo degradation of Congo Red (CR) under UV irradiation. UV-visible spectrums of Congo Red absorption ($\lambda = 500 \text{ nm}$) in the presence of the as-prepared samples (WO_3 nanoparticles and nanorods) illustrate in figure 6(a) and figure 6(b) respectively.

It was observed that by increasing the irradiation time, the maximum absorption peak decreases, which means that the concentration of Congo Red is decreasing in the presence of WO_3 nanostructures and UV illumination.

According to the figure 6(a) and figure 6(b), WO_3 nanoparticles with average size about 80 nm has better photo catalytic activity in comparison to another sample and according to the figure 6(c), in the case of WO_3 nanoparticles, the Congo Red photo degradation rate is more.

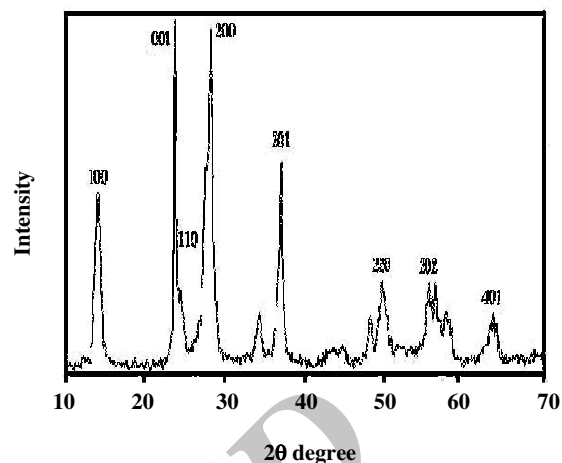


Fig. 5: XRD pattern of the as-prepared WO_3 nanorods that were prepared with modified hydrothermal method and indicates hexagonal structure.

We suppose that the observed difference between two morphologies of WO_3 nanostructures may be related to the growth direction and crystalline structure. Relaxation of atoms at the (001) WO_3 surface, causes a significant decrease of surface energy [28]. In comparison to the other faces, the great stability of (001) face, provides the best efficiency for the chemisorption and dissociation of oxygenated compounds at the WO_3 interface. According to the figure 7, the growth direction of the hexagonal WO_3 nanorods is only in one direction but in the case of WO_3 nanoparticles, it is the same in all directions and more crystalline planes may be aligned with (001) plane. Therefore, photo catalytic activity of WO_3 nanoparticles is better than WO_3 nanorods. However, the exact reason is not clear and needs further investigation in the future.

CONCLUSIONS

In this research, WO_3 nanoparticles were prepared by spray pyrolysis method. SEM image demonstrates uniform nanoparticles and XRD analysis illustrates the formation of WO_3 phase with monoclinic structure and average size about 80 nm.

WO_3 nanorods with hexagonal structure and average dimension about $15 \times 100 \text{ nm}$ were synthesized in gram quantities by modified hydrothermal method at lower temperature and shorter reaction time in comparison to the previous research [27].

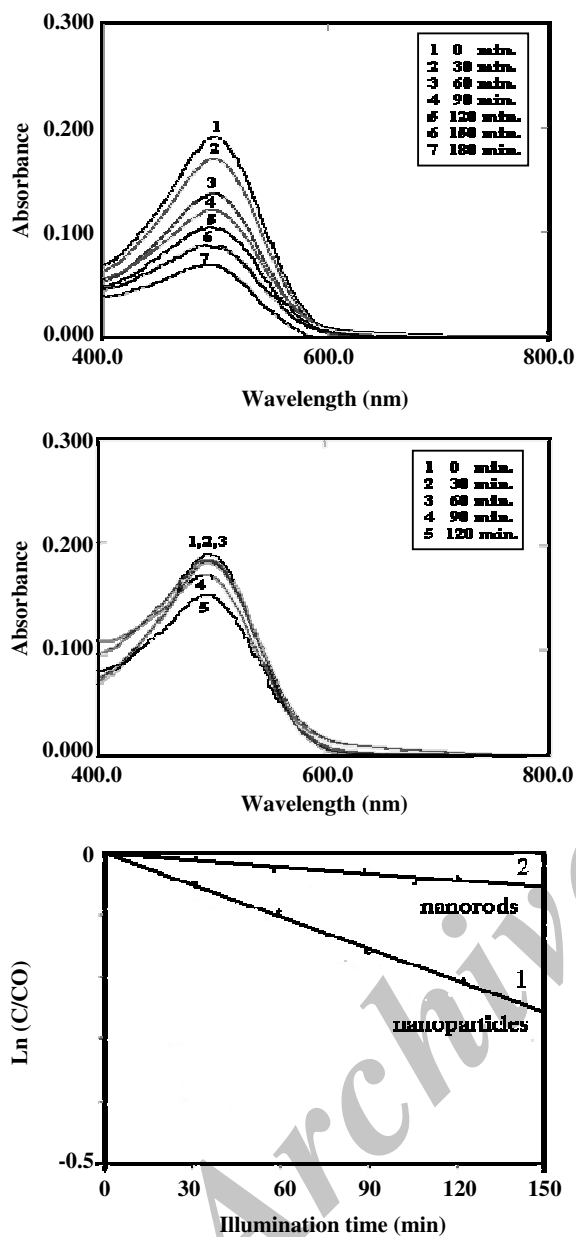


Fig.6: Evaluation of WO₃ nanostructures photo catalytic activity by Congo Red photo degradation. a: Congo Red aqueous solution with WO₃ nanoparticles with average size about 80 nm. b: Congo Red aqueous solution with WO₃ nanorods with average dimensions about 15 × 100 nm. c: Molecular structure of Congo Red. d: Change of Congo Red concentration versus the UV illumination time for samples 1: Congo Red aqueous solution with WO₃ nanoparticles with average size about 80 nm. 2: Congo Red aqueous solution with WO₃ nanorods with average dimensions about 15 × 100 nm.

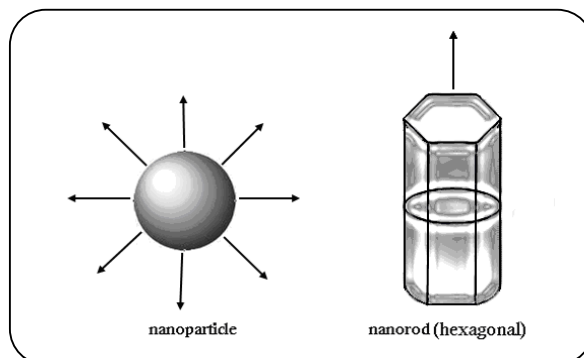


Fig. 7: Comparison between the growth direction of WO₃ nanoparticle and WO₃ nanorod.

The photo catalytic activity of WO₃ nanoparticles and WO₃ nanorods were measured by photo degradation of Congo Red under UV irradiation. The results show that, by increasing the irradiation time, the maximum absorption peak intensity and the concentration of Congo Red decreases in the presence of WO₃ nanoparticles and WO₃ nanorods. Results demonstrated that the photo catalytic activity of WO₃ nanoparticles is better than WO₃ nanorods. Therefore, in this reaction, spherical morphology is superior to column morphology

Received : Sep. 9, 2010 ; Accepted : May 16, 2011

REFERENCES

- [1] Hoffmann M.R., Martin S.T., Choi W., Bahnemann D.W., Environmental Applications of Semiconductor, *Chem. Rev.*, **95**, p. 69 (1995).
- [2] Machado A.E.H., Gomes A.J., Campos C.M.F. et al., Photoreactivity of Lignin Model Compounds in the Photobleaching of Chemical Publlps 2. Study of the Degradation of 4-Hydroxy-3-Methoxy-Benzadehyde and Two Lignin Fragments Induced by Singlet Oxygen, *J. Photochem. Photobiol. A*, **110**, p. 99 (1997).
- [3] Hagfeldt A., Graetzel M., Light-Induced Redox Reactions in Nanocrystalline Systems, *Chem. Rev.*, **95**, p. 49 (1995).
- [4] Schiavello M., Some Working Principles of Heterogeneous Photocatalysis by Semiconductors, *Electrochim. Acta.*, **38**, p. 11 (1993).
- [5] Hidaka H., Zhao J., Pelizzetti E., Serpone N., Photodegradation of Surfactants. Comparison of Photocatalytic Processes Between Anionic DBS and Cationic BDDAC on the Titania Surface, *J. Phys. Chem.*, **96**, p. 2226 (1992).

- [6] Matthews R.W., Photocatalytic Oxidation and Adsorption of Methylene Blue, *J. Chem. Soc., Faraday Trans.*, **185**, p. 1291 (1989).
- [7] Lakshmi S., Renganathan R., Fujita S., Study on TiO₂-Mediated Photocatalytic Degradation of Methylene Blue, *J. Photochem. Photobiol. A*, **88**, p. 163 (1995).
- [8] Singhal B., Porwal A., Sharma A., Ameta R., Ameta S.C., Photocatalytic Degradation of Cetylpyridinium Chloride Over Titanium Dioxide Powder, *J. Photochem. Photobiol. A*, **108**, 85 (1997).
- [9] Serpone N., Maruthamuthu P., Pichat P., Pelizzetti E., Hidaka H., Exploiting the Interparticle Electron Transfer Process in the Photocatalysed Oxidation of Phenol, 2-Chlorophenol and Pentachlorophenol: Chemical Evidence for Electron and Hole Transfer Between Coupled Semiconductors, *J. Photochem. Photobiol. A*, **85**, p. 247 (1995).
- [10] Vallejos S., Khatko V., Calderer J., Gracia I., Cane C., Llobet E., Correig X., Micro-Machined WO₃-Based Sensors Selective to Oxidizing Gases, *Sens. Actuators B*, **132**, p. 209 (2008).
- [11] Mitsugi F., Hiraiwa E., Ikegami T., Ebihara K., Pulsed Laser Deposited WO₃ Thin Films for Gas Sensor, *Surf. Coat. Technol.*, **169-170**, p. 553 (2003).
- [12] He X., Li J., Gao X., Wang L., NO₂ Sensing Characteristics of WO₃ Thin Film Microgas Sensor *Sens. Actuators B*, **93**, p. 463 (2003).
- [13] Ashirt P.V., Bader G., Truong V., Electrochromic Properties of Nanocrystalline Tungsten Oxide Thin Films, *Thin Solid Films*, **320**, p. 324 (1998).
- [14] Xu Z., Vetelino J.F., Lec R., Parker D.C., *J. Vac. Sci. Technol. A*, **8**, p. 3634 (1990).
- [15] Tagtstorm P., Jansson U., Chemical Vapour Deposition of Epitaxial WO₃ Films, *Thin Solid Films*, **352**, p. 107 (1999).
- [16] Haro-Poniaowski E., Jouanne M., Morhange J.F., Micro-Raman Characterization of WO₃ and MoO₃ Thin Films Obtained by Pulsed Laser Irradiation, *Appl. Surf. Sci.*, **127-129**, p. 674 (1998).
- [17] Lee S.H., Cheong H.M., Edwin C., Pitts J.R., Deb S.K., Alternating Current Impedance and Raman Spectroscopic Study on Electrochromic a-WO₃ Films, *Appl. Phys. Lett.*, **76**, p. 3908 (2000).
- [18] Lee D.S., Nam K.H., Lee D.D., Effect of Substrate on NO₂-Sensing Properties of WO₃ Thin Films Gas Sensors, *Thin Solid Films*, **375**, p. 142 (2000).
- [19] Cantalini C., Sun H.T., Faccio M. et al., NO₂ Sensitivity of WO₃ Tin Films Obtained by High Vacuum Thermal Evaporation, *Sens. Actuators B*, **31**, p. 81 (1996).
- [20] Cantalini C., Pelino M., Sun H.T. et al., Cross Sensitivity and Stability of NO₂ Sensors from WO₃ Thin Film, *Sens. Actuators B*, **35-36**, p. 112 (1996).
- [21] Moulzolf S.C., Ding S.An., Lad R.J., Stoichiometry and Microstructure Effects on Tungsten Oxide Chemiresistive Films, *Sens. Actuators B*, **77**, p. 375 (2001).
- [22] Kim T.S., Kim Y.B., Yoo K.S., Sung G.S., Jung H.J., Sensing Characteristics of dc Reactive Sputtered WO₃ Thin Films as an NO_x Gas Sensor, *Sens. Actuators B*, **62**, p. 102 (2000).
- [23] Penza M., Tagliente M.A., Mirengi L., Gerardi C., Martucci C., Cassano G., Tungsten Trioxide (WO₃) Sputtered Thin Films for a NO_x Gas sensor, *Sens. Actuators*, **50**, p. 9 (1998).
- [24] Tagtstorm P., Jansson U., Chemical Vapour Deposition of Epitaxial WO₃ Films, *Thin Solid Films*, **352**, p. 107 (1999).
- [25] Vijayalakshmi J., Jayachandran M., Sanjeeviraja C., Structural, Electrochromic and FT-IR Studies on Electrodeposit Tungsten Trioxide Films, *Curr. Appl. Phys.*, **3**, p. 171 (2003).
- [26] Cantalini C., Wlodarski W., Li Y., Passacantando M., Santucci S., Comini E., Faglia G., Sberveglieri G., Investigation on the O₃ Sensitivity Properties of WO₃ Thin Films Prepared by Sol-Gel, Thermal Evaporation and r.f. Sputtering Techniques, *Sens. Actuators B*, **64**, p. 182 (2000).
- [27] Therese H.A., LI J., Kolb U., Tremel W., Facile Large Scale Synthesis of WS₂ Nanotubes from WO₃ Nanorods Prepared by a Hydrothermal Route, *Solid State Sci.*, **7**, p. 67 (2005).
- [28] Alaei M., Rashidi A.M., Mahjoub A., Two Suitable Method for the Preparation of Inorganic Fullerene-Like (IF) WS₂ Nanoparticles, *Iran. J. Chem. Chem. Eng. (IJCCE)*, **50**, p. 91 (2009).
- [29] Mpouretedal H.R., Keshavarz M.H., Yosefi M.H., Shokrollahi A., Zali A., Photodegradation of HMX and RDX in the presence of Nanocatalyst of Zinc Sulfide Doped with Copper, *Iran. J. Chem. Chem. Eng. (IJCCE)*, **53**, p. 13 (2009).